

PART - III

CHAPTER – 8

MICRO HARDNESS OF $\text{InBi}_{1-x}\text{Sb}_x$ AND $\text{InBi}_{1-x}\text{Se}_x$ SINGLE CRYSTALS

CHAPTER – 8

MICROHARDNESS OF $\text{InBi}_{1-x}\text{Sb}_x$ AND $\text{InBi}_{1-x}\text{Se}_x$ SINGLE CRYSTALS

The results of microhardness studies on $\text{InBi}_{1-x}\text{Sb}_x$ and $\text{InBi}_{1-x}\text{Se}_x$ are included in this chapter. Microhardness indentation tests were carried out on the cleavage planes (001) of the $\text{InBi}_{1-x}\text{Sb}_x$ and $\text{InBi}_{1-x}\text{Se}_x$ crystals by using the Vickers diamond pyramidal indenter. The study includes hardness variation with applied load, time and azimuthal orientation of indenter. Effects of cold working and crystal perfection on hardness have also been studied.

INTRODUCTION :

The indentation method is the most widely used method for measurement of hardness of the crystals either of metallic or nonmetallic nature. This method does not require large specimens and even on a small specimen a number of measurements can be carried out. Among the various factors on which the measured value of hardness depends, friction and prior strain hardening also depends on the geometry of the indenter. The indenter used must be either sharp or blunt according to their included angles which are less or greater than 90° . As this angle increases, the indenter tends to be blunt and influence of friction and prior strain hardening decreases. Also, the value of the constraint factor “C” in the

relation between hardness and yield stress ($H = CY$), tends to 3 as the effective cone angle increases (Shaw)⁽¹⁾. The stress field produced by such an indenter closely approximates to the prediction of elastic theory. The Vickers diamond pyramidal indenter used in the present study has the included angle of 136° which is a good compromise to minimize frictional effects and at the same time to give a well defined geometrically shaped indentation mark. Also during the diamond contact with the cleavage surface of a metal, the coefficient of friction ranges from 0.1 to 0.15 making the frictional effects less pronounced (Tabor)⁽²⁾. The Vickers hardness is defined as the ratio of applied load to the pyramidal contact area of indentation and it is calculated as

$$H_v = \frac{1854 \times 9.8 \times P}{d^2} \quad \text{MPa} \quad \dots\dots (1)$$

where,

H_v = Vickers microhardness in MPa

P = applied load in mN

d = mean diagonal length of the indentation mark in μm

The indentation mark is geometrically similar whatever its size. This would imply the hardness to be independent of load. However, this is not the case and except for loads exceeding about 200 gm (i.e. 1960 mN) in general, the measured hardness value has been found to depend on load in almost all cases and hence the hardness values measured in the low load region ($< 200\text{gm}$. i.e., $< 1960\text{ mN}$), are known

as microhardness values. Though, the limit load is not sharply defined and practically the hardness may achieve a constant value for loads in the range 20 to 50 gm (i.e., 196 to 490 mN) and beyond, depending on the material.

In general, the nature of variation of hardness with load is quite complex and does not follow any universal rule. Many workers have studied the load dependence of hardness and the results obtained are quite confusing. As for example Bergsman observed a very pronounced load dependence of hardness⁽³⁾. The load variation of hardness was studied by Rostoker⁽⁴⁾ in the case of copper and observed a decrease in hardness at low applied loads. In contrast to this, a considerable increase in the hardness values at low applied loads was observed by Buckle⁽⁵⁾. This increase in the hardness value has been observed due to elastic recovery after removing the applied load which reduces the diagonal length. For sintered carbides, Grodzinsky⁽⁶⁾ found that the plot of hardness versus load shows a peak at low applied loads. Knoop et al⁽⁷⁾ and Bernhardt⁽⁸⁾ found the increase in the hardness value with decreasing load. On the other hand, Campbell et al⁽⁹⁾ and Mott et al⁽¹⁰⁾ observed a decrease in hardness with decrease in load. Whereas, Taylor⁽¹¹⁾ and Toman et al⁽¹²⁾ have reported no significant change in the hardness value with variation of load. Such contradictory results^(5 - 13) may be due to the effects of the surface layers and vibrations produced during the work. Gane et al⁽¹⁴⁾

studied the microhardness at very small loads. They observed a sharp increase in hardness at small indentation sizes and suggested that this increase may be due to the high stresses required for homogeneous nucleation of dislocations in the small dislocation free regions indented. On the contrary, Ivan'ko⁽¹⁵⁾ found a microhardness decrease with decreasing load and concluded that this dependence is due to the relative contributions of plastic and elastic deformations in the indentation process.

According to these different observations and reports, it can be said that it is difficult to establish any definite relationship between microhardness and applied load. As shown in equation 1, the hardness to be independent of load P should be directly proportional to the square of the diagonal length “ d ”. Thus,

$$P = ad^2 \dots\dots\dots (2)$$

where “ a ” is a material constant. This equation is known as Kick's law. According to the above discussion, the observed hardness dependence on load implies that the power index in this equation should differ from 2 and according to Hanemann⁽¹⁶⁾, the general form of dependence of load on the diagonal length should be in the form of

$$P = ad^n \dots\dots\dots (3)$$

Here, the dependence of hardness on load reflects in the deviation of the value of the index ‘ n ’ from 2. Thus, this equation is an analytical means

to study hardness variation with load. The exponent ‘n’ in the equation is also known as Meyer index or logarithmic index. Hanemann⁽¹⁶⁾ observed and concluded that in the low load region, ‘n’ generally has a value less than 2, which accounts for the higher hardness at low loads. However, Mil’vidskii et al⁽¹⁷⁾ observed the value of “n” in the range from 1.3 to 4.9.

The load dependence of hardness in low load range is thus inevitable. There have been reports of increase of hardness with load in this range. It is also found that the hardness in any case reaches a constant value for a range of high loads. Boyarskaya⁽¹⁸⁾ correlated the increase of hardness with load to the penetrated surface layers and the dislocation content in the case of polished and natural faces of NaCl single crystals. In the case of aluminum and magnesium single crystals, Yoshino⁽¹⁹⁾ observed that the microhardness increased rapidly first with the increasing load and then decreased gradually and finally became independent of load. The decrease in hardness with load is attributed to the heterogeneous deformation and anisotropy.

In the present work on $\text{InBi}_{1-x}\text{Sb}_x$ and $\text{InBi}_{1-x}\text{Se}_x$ single crystals grown by the zone melting method after 8 zone levelling passes at the growth speed of 1 cm/hr were used for the microhardness study and the results are discussed below.

All indentation tests were carried out on cleavage surfaces of the crystals. The samples were in the form of at least 3 to 4 mm thick slices.

The indentations were made on freshly cleaved surfaces in all the cases. To avoid unwanted anisotropic variations in the measured hardness it is necessary to keep constant the azimuthal orientation of the indenter with respect to the crystal surface. So to fix this orientation the samples used for the tests were etched at their corners in the dislocation etchant for delineating the crystallographic direction $[110]$ [Chapter - 7]. The first trial indentation was used to orient the diagonal of the indentation mark parallel to this direction. Subsequent indentations were then made keeping this orientation constant. For each measurement three indentations were made and average diagonal length was used for calculating hardness.

VICKERS HARDNESS STUDY OF $\text{InBi}_{1-x}\text{Sb}_x$ AND $\text{InBi}_{1-x}\text{Se}_x$ CRYSTALS :

The indentations were performed at a very slow rate and for all indentations care was taken to see that the rate was nearly the same. Also, between two neighboring indentation marks on the same surface, a separation of at least three indentations was maintained to avoid interference. The indentation mark was square in shape (Fig.1). The diagonals of indentation mark were measured using micrometer eyepiece with least count 0.19 micron.

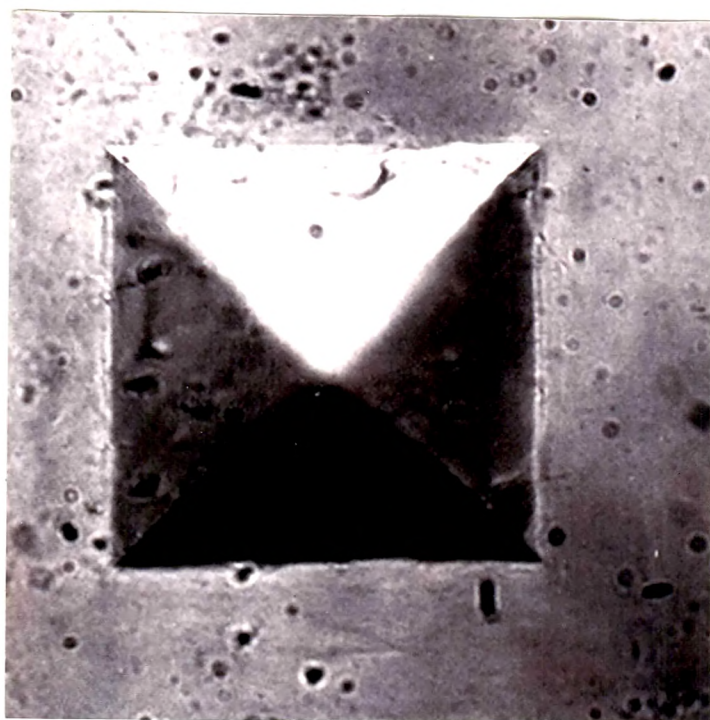


Fig. 1

To decide the indentation time to be kept constant during the hardness measurements at room temperature, the experiments were performed for various indentation times from 5 seconds to 100 seconds keeping applied load constant at 50 gm (i.e., 450 mN). This load is sufficiently a high load at which the hardness was observed to be insensitive to small load variations. Fig.2 and Fig.3 are the plots of H_v versus t for $\text{InBi}_{0.8}\text{Sb}_{0.2}$ and $\text{InBi}_{0.8}\text{Se}_{0.2}$ crystals respectively. From these plots, it can be seen that the hardness value is high for small indentation time. As the indentation time increases, the hardness decreases and tends to become constant for indentation time ≥ 30 second and ≥ 50 second in the case of $\text{InBi}_{0.8}\text{Sb}_{0.2}$ and $\text{InBi}_{0.8}\text{Se}_{0.2}$ single crystals, respectively. Hence indentation times of 30 and 50 seconds were kept constant to study other hardness variation, respectively, for $\text{InBi}_{0.8}\text{Sb}_{0.2}$ and $\text{InBi}_{0.8}\text{Se}_{0.2}$. The results are discussed below.

VARIATION OF HARDNESS WITH LOAD :

The indentations using Vickers pyramidal diamond indenter were made at different loads ranging from 5 mN to 1000 mN for fixed azimuthal orientations of the indenter to avoid anisotropic variation as described earlier. The indentation time was kept constant at 30 second and 50 second, respectively, for $\text{InBi}_{1-x}\text{Sb}_x$ and $\text{InBi}_{1-x}\text{Se}_x$ crystals.

$\text{InBi}_{0.8}\text{Sb}_{0.2}$

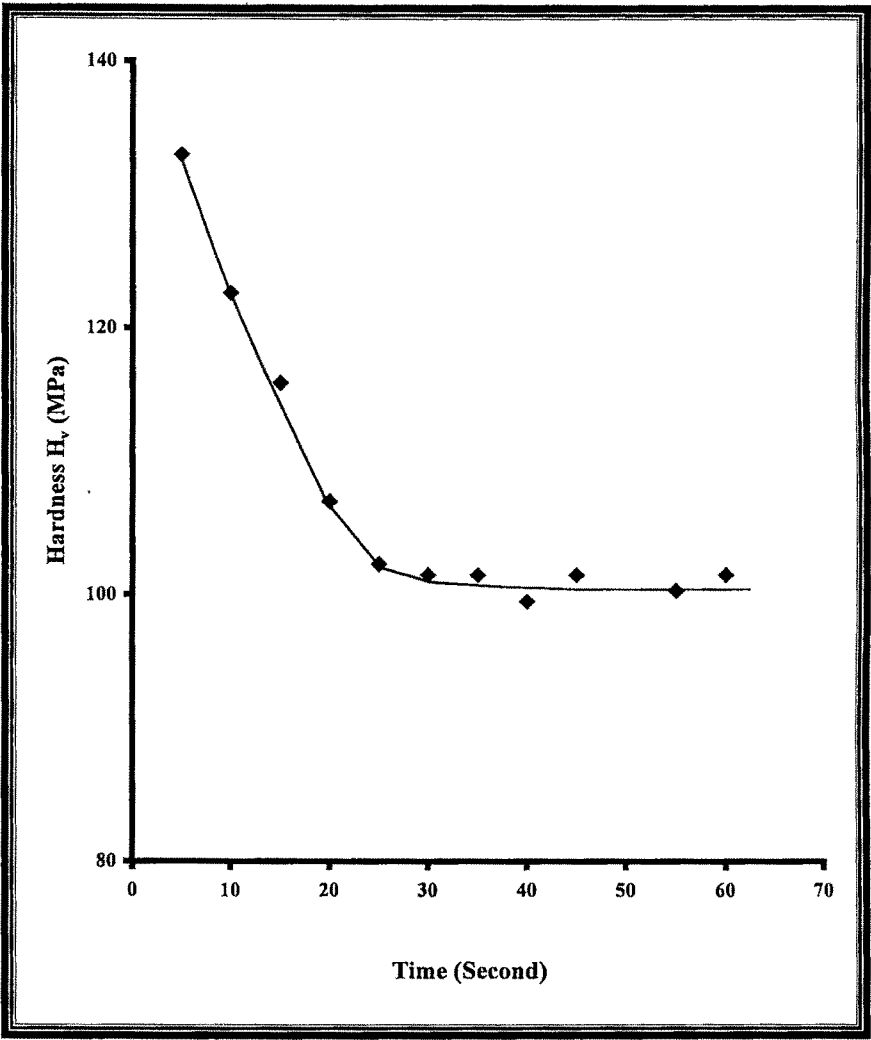


Fig. 2

$\text{InBi}_{0.8}\text{Se}_{0.2}$

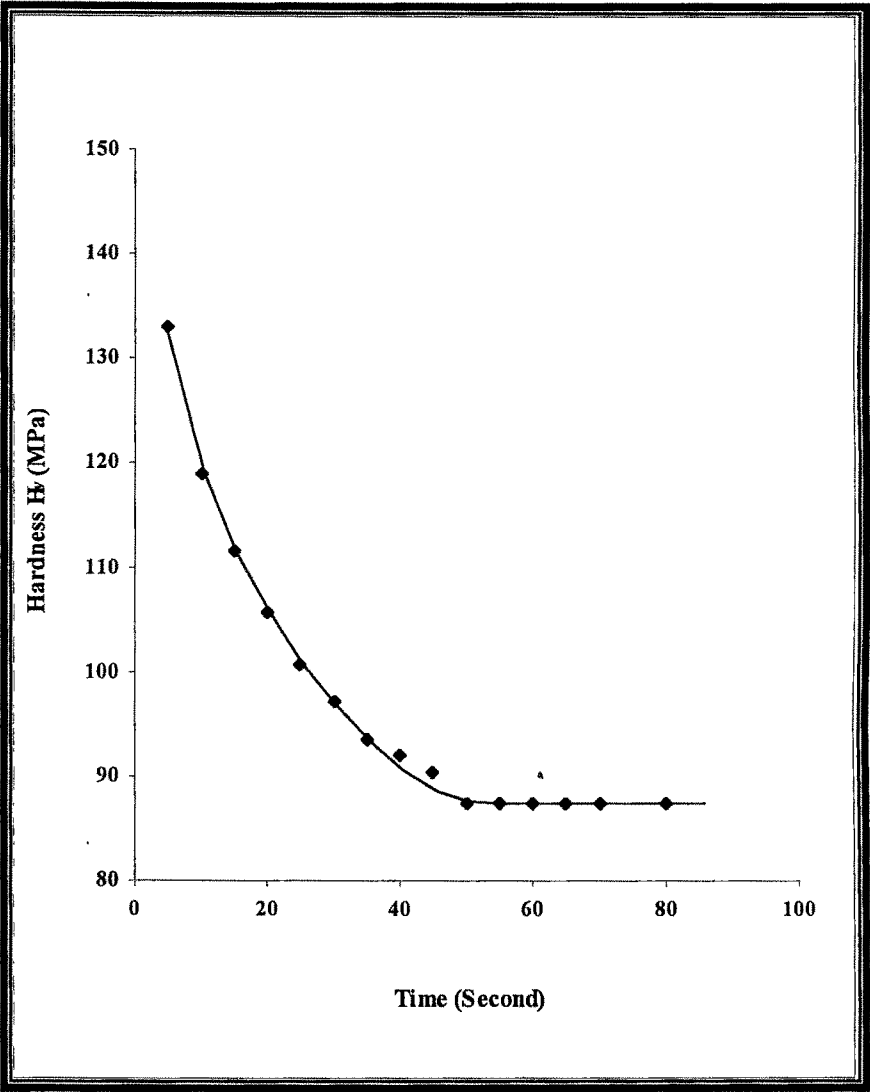


Fig. 3

Fig 4. shows the plot of Vickers hardness H_v versus load P , obtained at room temperature, for $\text{InBi}_{1-x}\text{Sb}_x$ (where $x = 0.2, 0.3, 0.4$). Fig. 5 represents similar plots for the $\text{InBi}_{1-x}\text{Se}_x$ crystal (where $x = 0.2, 0.3, 0.4$). The plots indicate clearly that the hardness varies with load in a complex manner. Increase in hardness at low load values is a common feature observed in all the plots. The hardness reaches a peak and displays complex variation with increase in load and becomes constant at sufficiently high loads as can be seen from the plots.

In general the hardness varies considerably in the low load region as the work hardening capacity and elastic recovery of a particular material are dependent on the load, type of surface receiving the load and the depth to which the surface is penetrated by the indenter. For example, the low load hardness behavior in the case of silicon single crystal has been explained on the basis of elastic recovery and piling up of material around the indentation mark (Walls et al)⁽²⁰⁾. Both the magnitude of work hardening and the depth to which it occurs depend on the properties of the material and are the greatest for soft metallic materials which can be appreciably work hardened. Since the penetration depth at high loads is usually greater than that of the work hardened surface layer, the hardness value at high loads will be representative of the undeformed bulk of the material and hence independent of load. Even for surfaces which require no mechanical preparation, e.g., cleavage faces of metals and minerals,

$\text{InBi}_{1-x}\text{Sb}_x$ (as cleaved)

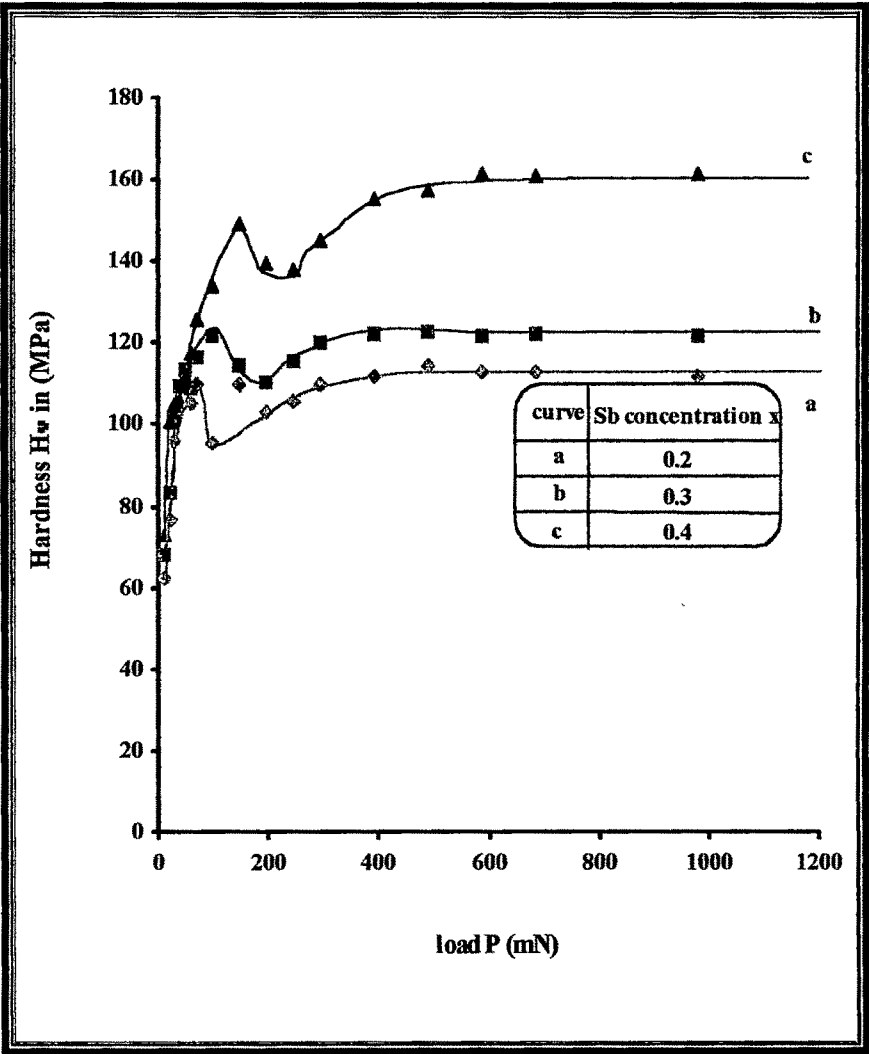


Fig. 4

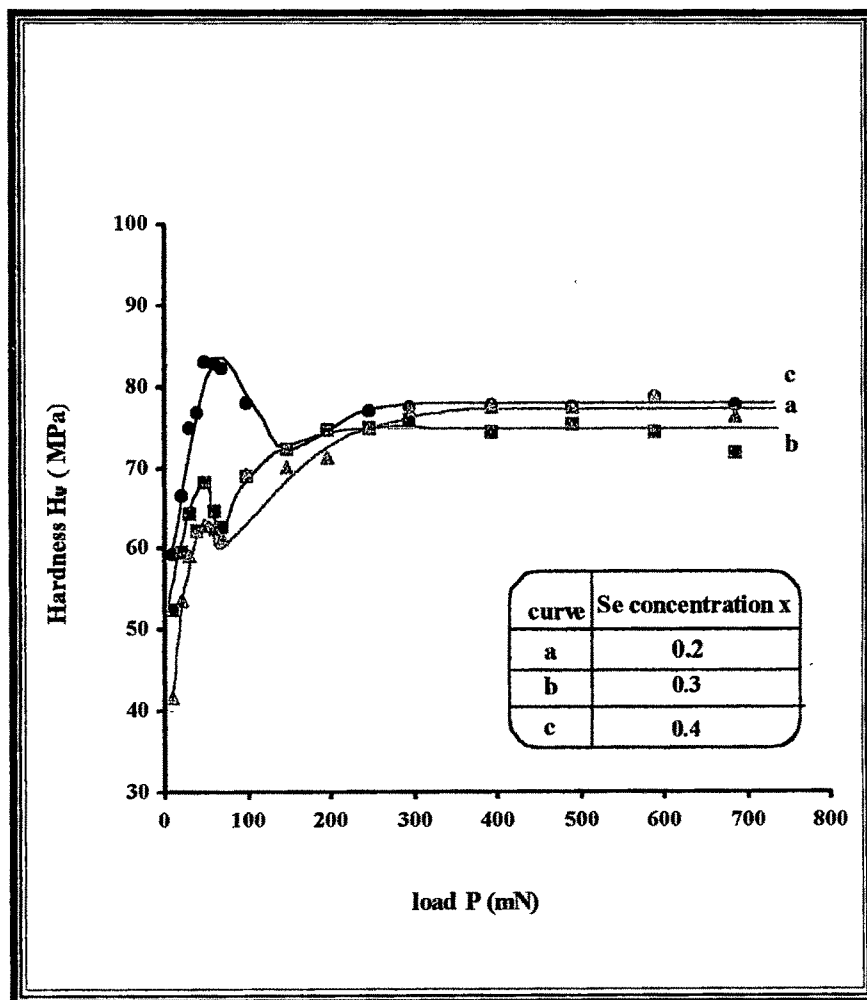
$\text{InBi}_{1-x}\text{Se}_x$ (as cleaved)

Fig. 5

the hardness obtained at small loads may not still be the same at high loads.

Now the depth of penetration depends usually on three factors:

- [1]. The type of surface receiving the load which can again be divided in to three categories :
 - (a). surface layers having different degrees of cold working (Onitsch)⁽²¹⁾
 - (b). surface layer having finely precipitated particles (Buckle)⁽²²⁾ and
 - (c). surface layer having different grain size (Bochvar et al)⁽²³⁾ and number of grains indented (Onitsch)⁽²⁴⁾, if the specimen is a polycrystal.
- [2]. The magnitude of the applied load and
- [3]. Accuracy in the normal operation of indenting the specimen and the rate at which the indentation is carried out, i.e., the strain rate. The time taken to realize the full load will evidently decide the strain rate.

All these factors play a prominent role when hardness tests are carried out by indentation at low loads. On the basis of depth of penetration of the indenter the observed variation of hardness with load in the plot of H_v v/s P may be explained. At small loads, the indenter pierces only surface layers and hence the effect is more prominent at those loads.

As the depth of penetration increases with load, the effect posed by the surface layers of the crystal becomes less sharp which makes the variation of microhardness with load less prominent at higher applied loads. After certain depth of penetration, the effect of inner layers becomes more and more prominent than those of the surface layers and ultimately there is practically no change in the hardness value with load.

The surface – layer – sensitive initial increase in hardness with load can be explained in terms of strain hardening based on dislocation theory. It is known that dislocations are surrounded by elastic stress fields. The stress fields of different dislocations interact strongly and lock the dislocations into metastable configurations. The effect becomes quite pronounced in metals where the dislocation mobility is usually high and the individual dislocations move readily at much lower stresses. The flow that occurs during indentation is therefore not limited by drag on isolated dislocations. The interactions between dislocations create jogs on them and these jogs create trails of dislocation dipoles behind the moving dislocations. As the penetration proceeds, the structure soon becomes filled with interacting dislocations forming complex networks resulting into efficient barriers to the motion of new and existing dislocations. Further flow is then limited by the strength of interactions between the barriers and dislocations. The externally applied stress required to produce further plastic deformation must be sufficient to make the

dislocations move through the opposing stress field of these interactions. The effective dislocated zones in the damaged layer causing such back stresses may correspond to what are known as “coherent regions” (Buckle)⁽²⁵⁾.

Thus, the bulk characteristic hardness is usually represented by the value in the saturation region. The results in the present case can be summarized as in Table-1 which lists the constant hardness values obtained from these plots together with the dislocation densities of crystals with different Sb and Se concentrations, respectively. The hardness obtained from these data is plotted in Fig.6 and Fig.7 as a function of Sb and Se concentrations, respectively.

It can be seen that in the case of $\text{InBi}_{1-x}\text{Sb}_x$, the hardness shows about 45 % increase with x increasing from 0.2 to 0.5, whereas in the case of $\text{InBi}_{1-x}\text{Se}_x$, the hardness is practically independent of concentration of Se. This should imply that Sb might be going into substitutional position of Bi. It may be noted that Bi and Sb radii are equal within 10 % whereas Se is smaller than Bi by about 20 %. Thus Se atoms may go into interstitial position rather than substitutional. Further the pure InBi crystal has been reported to have the Vicker's hardness about 10 Kg/mm^2 . Thus addition of Sb/Se has very significantly increased the crystal hardness.

Table – 1

Sb/Se Concentration X	As cleaved InBi _{1-x} Sb _x		As cleaved InBi _{1-x} Se _x	
	Dislocation density (cm ⁻²)	Hardness H _v (MPa)	Dislocation density (cm ⁻²)	Hardness H _v MPa)
0.2	2 x 10 ⁴	113	2.5 x 10 ⁴	78
0.3	3 x 10 ⁴	122	3.5 x 10 ⁴	75
0.4	4 x 10 ⁴	161	4.5 x 10 ⁴	77.5

$\text{InBi}_{1-x}\text{Sb}_x$

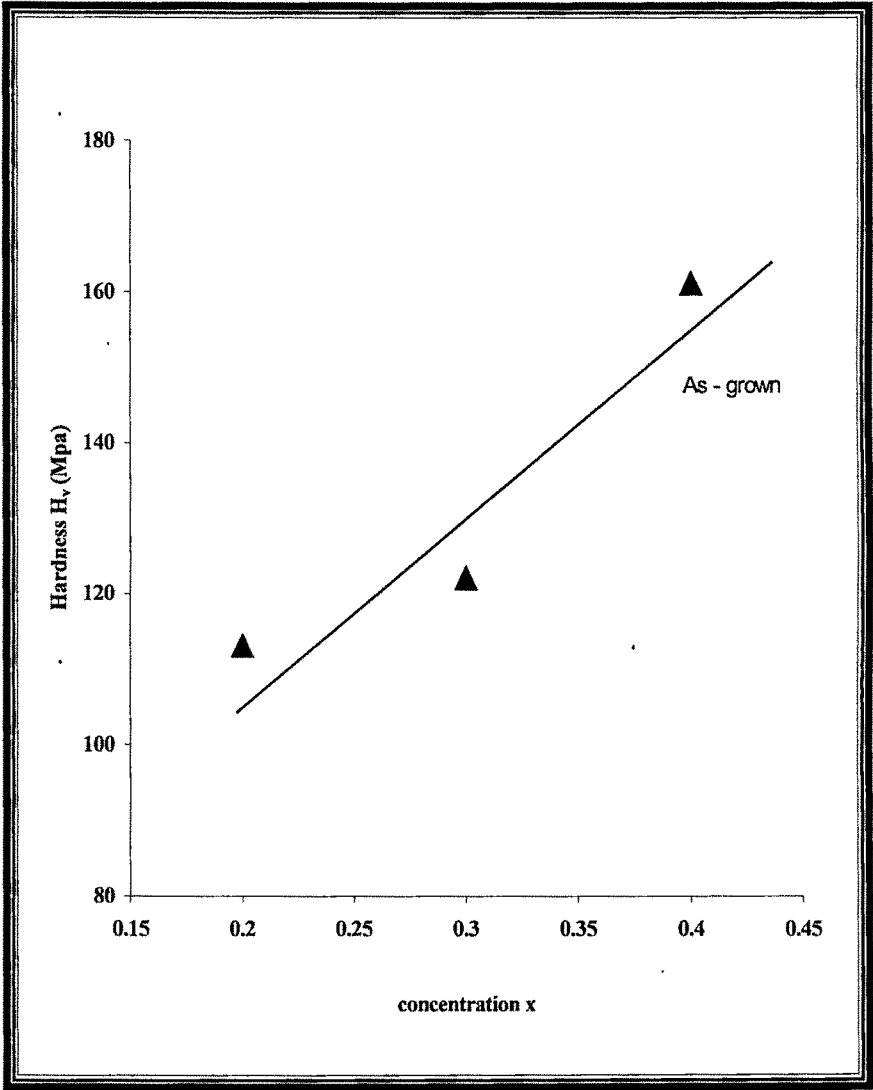


Fig. 6

$\text{InBi}_{1-x}\text{Se}_x$

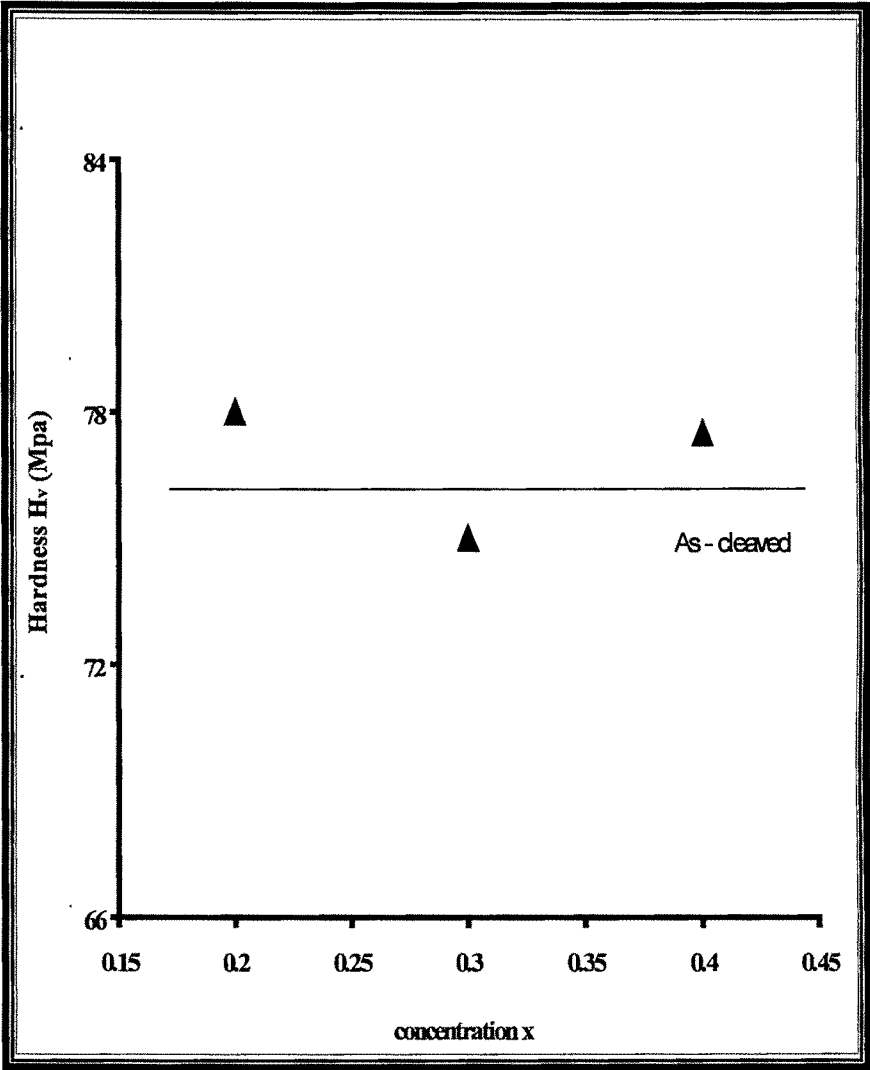


Fig. 7

EFFECT OF ZONE – LEVELLING PASSES :

$\text{InBi}_{0.8}\text{Sb}_{0.2}$ and $\text{InBi}_{0.8}\text{Se}_{0.2}$ single crystals were also grown using large number of zone levelling passes, namely 30, and their hardnesses were measured in identical conditions. From Fig – 8 and Fig – 9 it can be seen that as the number of alternate zone passes increases, from 8 to 30, the load independent hardness decreases. It is known that the perfection of the crystal increases due to improved homogeneity of the crystals as a result of large number of passes (Pfann, W.G.)⁽²⁶⁾. From above plots it can also be seen that peak has disappeared in the case of 30 zone passes. Although, the load dependence in the low load range persists. The disappearance of the peak may be caused by suppression of the coherent region due to improved perfection of the crystal (Buckle, H.; Braunovic.; Vyas S.M. et al.; Jani et al)^(27- 30).

The effect can be plausibly explained on the basis of deformation induced coherent regions, which incorporate the complexities of strain hardening. The presence of coherent regions has also been evidenced clearly by the depth profile of dislocation etchpit distributions below the indentations in the case of silver single crystal, (Chen and Hendrickson)⁽³¹⁾. The coherent regions in the present case accordingly extend to the depth of penetration of the indenter under the loads corresponding to the hardness peaks. Thus the increase in hardness with load in the low load range gets limited by the extent of the coherent

$\text{InBi}_{1-x}\text{Sb}_x$

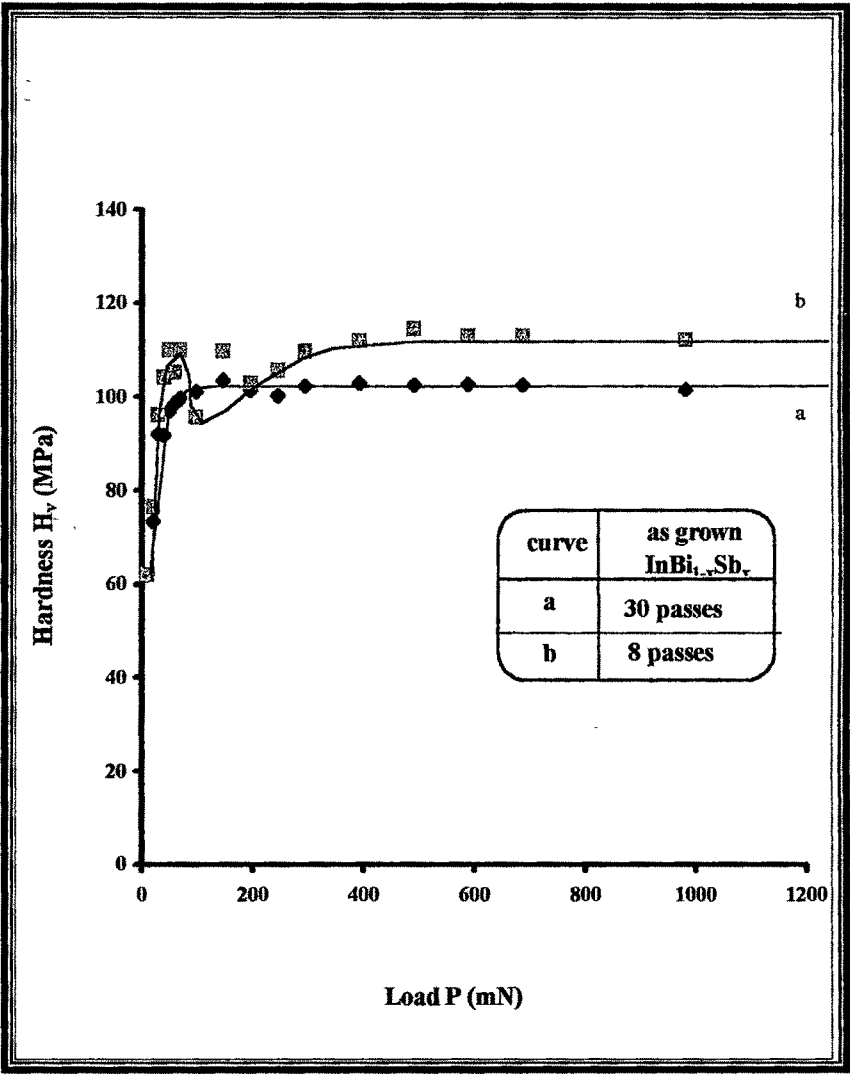


Fig. 8

$\text{InBi}_{1-x}\text{Se}_x$

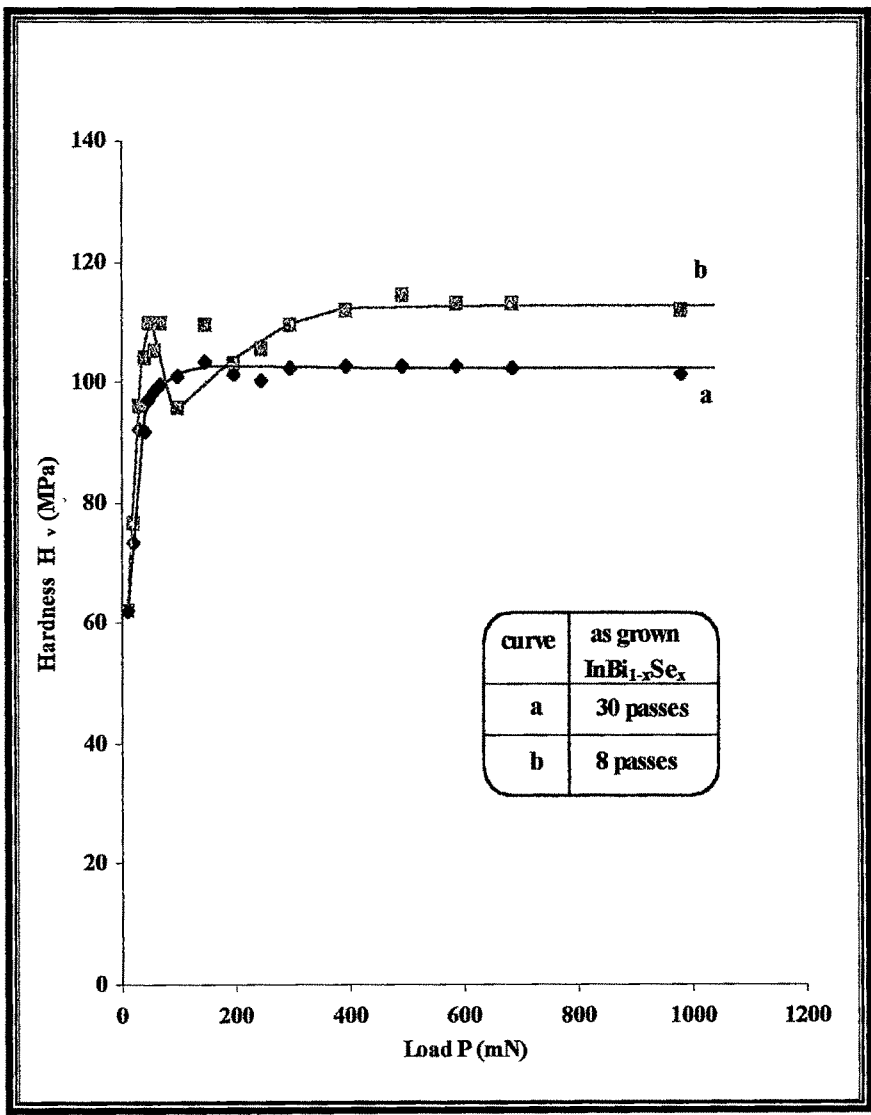


Fig. 9

region. The disappearance of the hardness peaks may be thus due to the corresponding disappearances of the coherent regions caused by improved crystal perfection. The dislocation density measurements on the crystals grown by 8 passes and by 30 passes indicate the improved perfection, with increased number of passes as discussed in Chapter-6.

EFFECT OF COLD WORKING :

To study the effect of work hardening on the load dependence of hardness, the crystals were cold worked prior to indentation. For this purpose 5 to 6 mm thick cleaved plates of the crystals were placed between two flat glass slabs and a load of about 3 kg was placed over the top slab. This effectively produced compression along the 'C' axis of the crystals and compression was continued for 24 hr. at room temperature. Then the crystals were cleaved to obtain one to two mm thick slices and the Vickers indentations were carried out at different loads. This experiment was repeated on several samples with identical treatment.

Fig. 10 and Fig.11 show average results of dependence of hardness H_v on applied load P for both the crystals, respectively.

Due to the cold working on the samples the load independent hardness has also increased to a considerable extent Table – 2 and Table – 3 indicate this, respectively, for $\text{InBi}_{1-x}\text{Sb}_x$ and $\text{InBi}_{1-x}\text{Se}_x$ crystals.

$\text{InBi}_{1-x}\text{Sb}_x$ (cold worked)

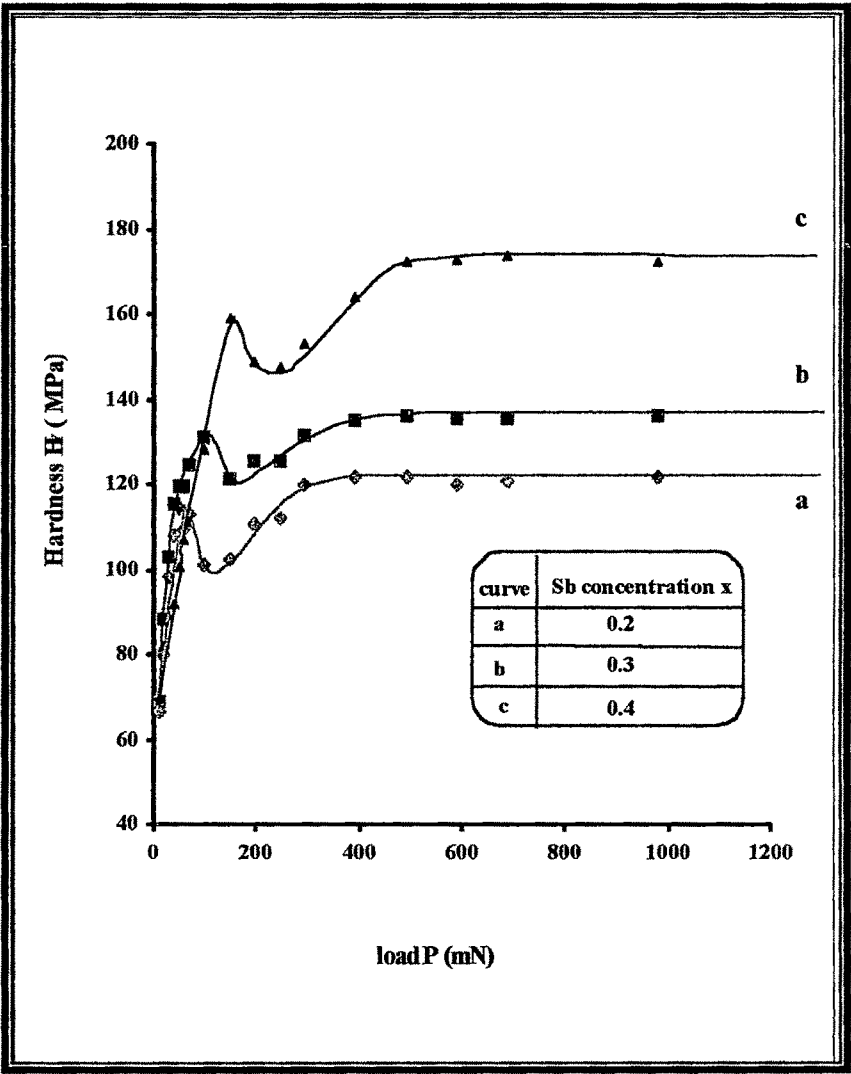


Fig. 10

$\text{InBi}_{1-x}\text{Se}_x$ (cold worked)

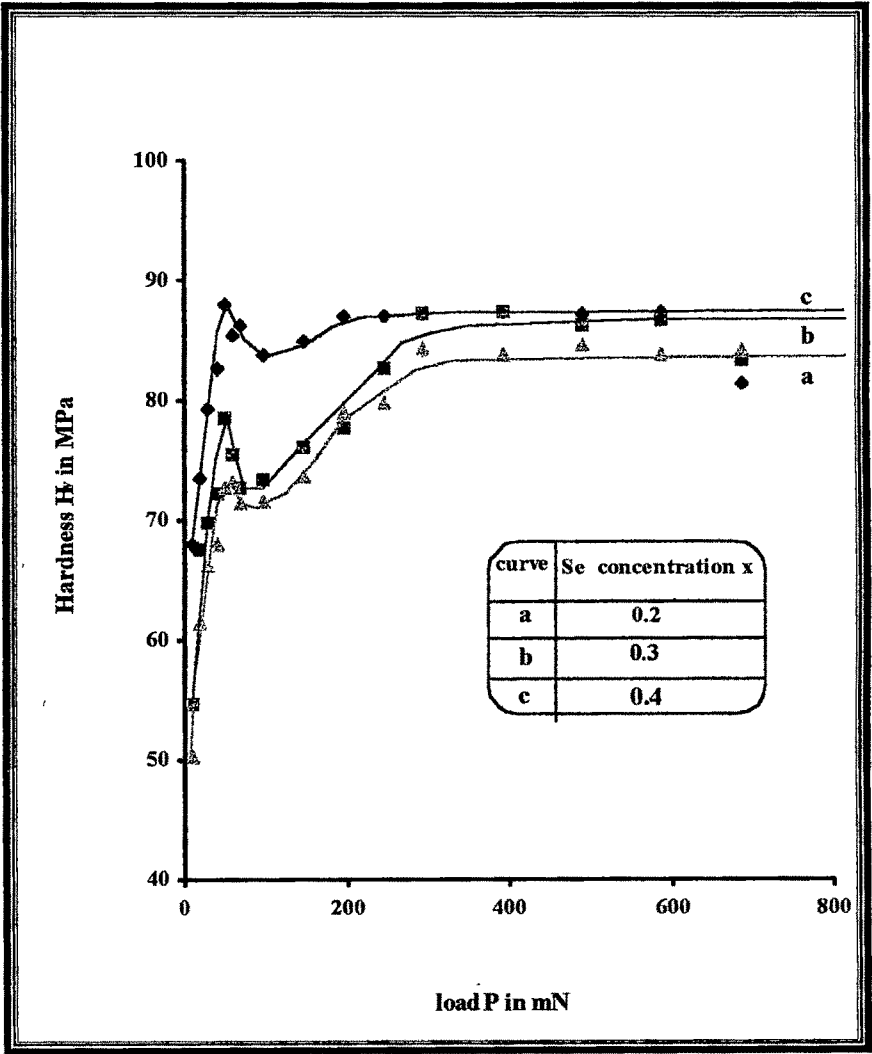


Fig.11

Table – 2

$\text{InBi}_{1-x}\text{Sb}_x$			
Concentration x	As grown H_v (MPa)	Cold worked H_v (MPa)	% rise in hardness
0.2	113	122	8
0.3	122	136	11.5
0.4	161	172.5	7

Table – 3

$\text{InBi}_{1-x}\text{Se}_x$		
Concentration x	As grown Hv (MPa)	Cold worked Hv (MPa)
0.2	78	87
0.3	75	87
0.4	77.5	84

The Meyer's law is useful to analyze dependence of hardness on load. This law is $P = ad^n$.

where,

n is known as Meyer's index,

P is the applied load,

d is the diagonal length of the indentation mark and

a is the material constant.

The deviation of the value of n from 2 reflects the load dependence of hardness⁽³²⁾. The Meyer's law can be written as $\log P = \log a + n \log d$.

Using the data of d v/s P , $\log P$ v/s $\log d$ plots were obtained.

Fig.12(a), (b) and (c) show the plots of $\log P$ v/s $\log d$ for as cleaved $\text{InBi}_{1-x}\text{Sb}_x$ (where $x = 0.2, 0.3, 0.4$) crystals and Fig.13(a), (b) and (c) represent the plots of $\log P$ v/s $\log d$ for as cleaved $\text{InBi}_{1-x}\text{Se}_x$ (where $x = 0.2, 0.3, 0.4$) crystals. Similarly, Fig.14(a), (b) and (c) and fig.15(a), (b) and (c) represent the plots of $\log P$ v/s $\log d$ for cold worked crystals of $\text{InBi}_{1-x}\text{Sb}_x$ and $\text{InBi}_{1-x}\text{Se}_x$ (where $x = 0.2, 0.3, 0.4$) crystals. It can be seen that the plots exhibit a straight line nature. The slope of the straight lines indicate the value of Meyer index n . Almost all of these values show deviations from ideal 2. Such variations in the Meyer index have been reported for steel and soft iron (O' Neill)⁽³³⁾, for tellurium (Trivedi)⁽³⁴⁾ etc.

$\text{InBi}_{0.8}\text{Sb}_{0.2}$ (as cleaved)

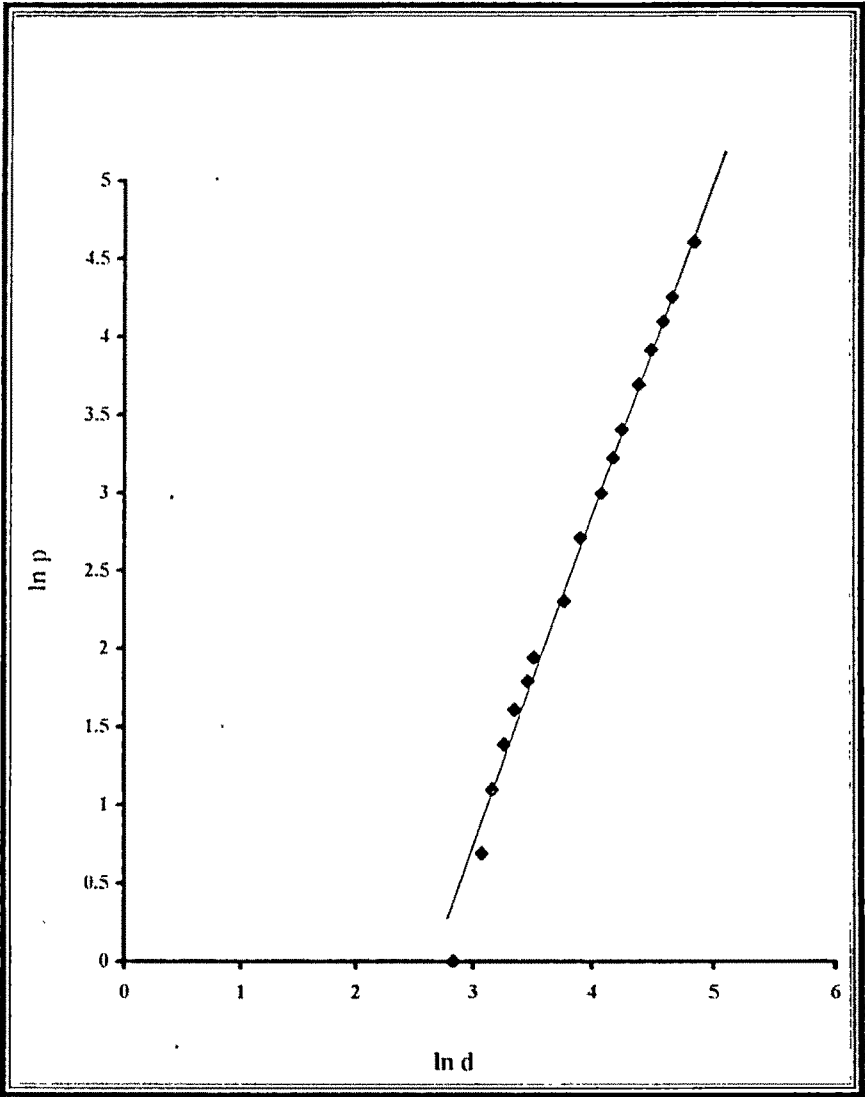


Fig. 12(a)

$\text{InBi}_{0.7}\text{Sb}_{0.3}$ (as cleaved)

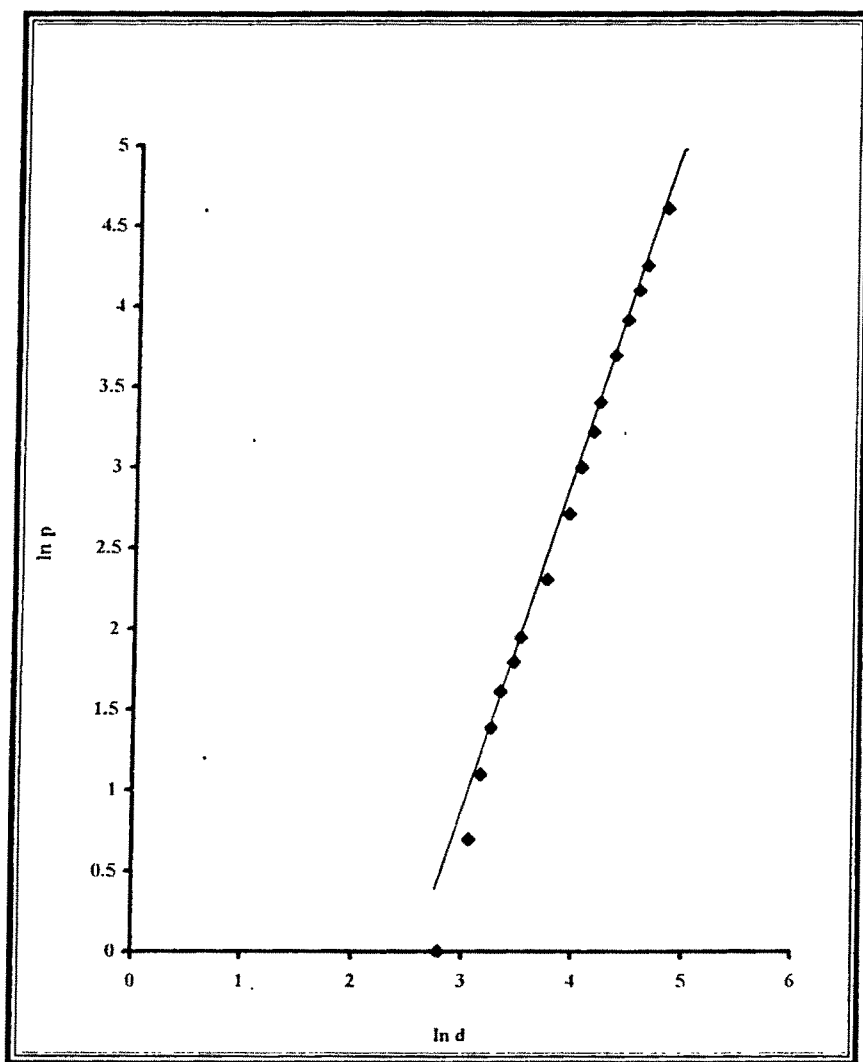


Fig. 12(b)

$\text{InBi}_{0.6}\text{Sb}_{0.4}$ (as cleaved)

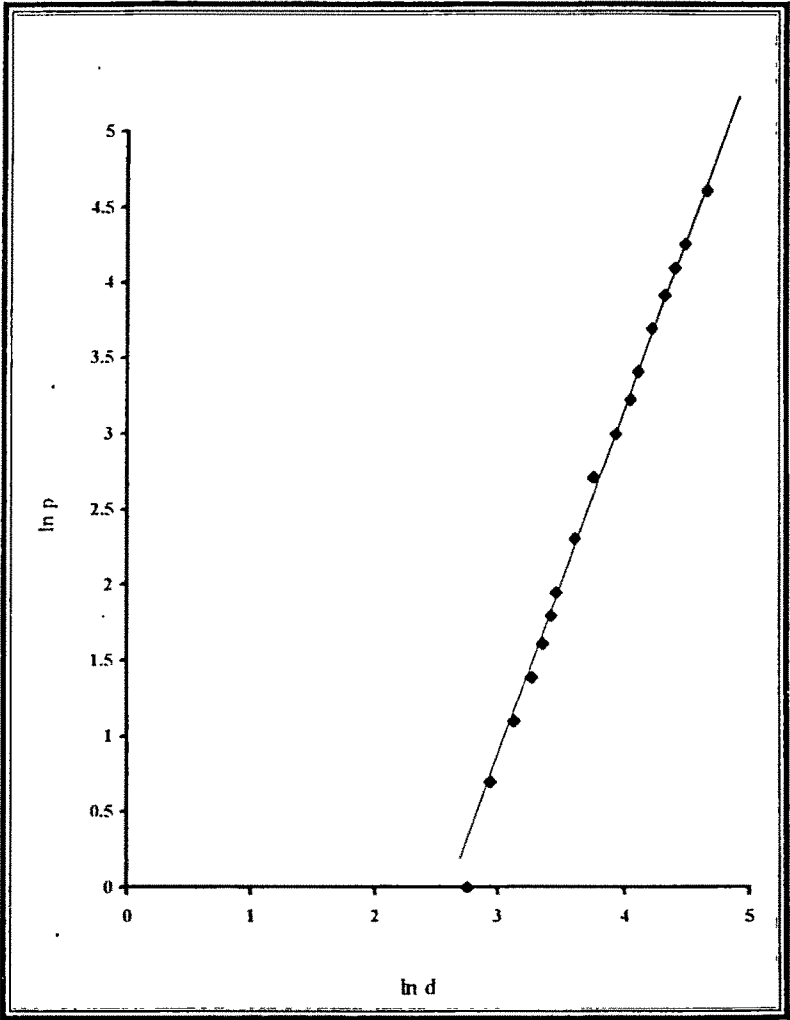


Fig. 12(c)

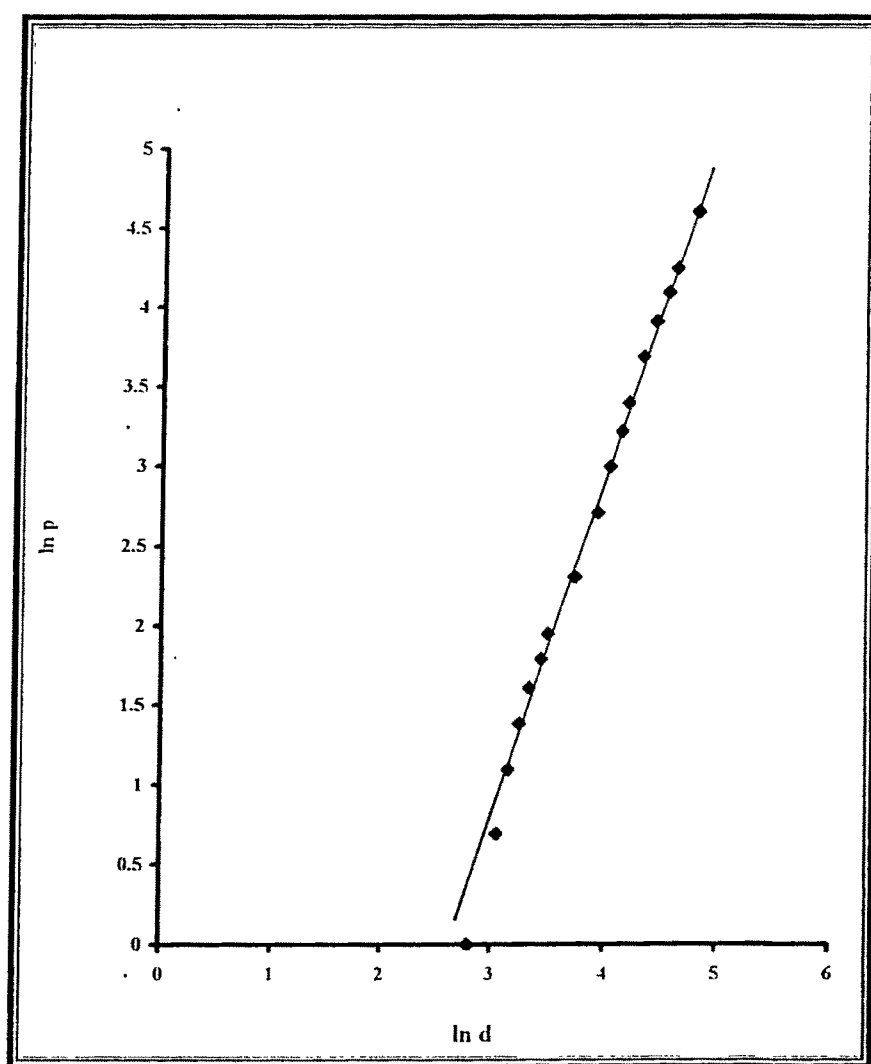
$\text{InBi}_{0.8}\text{Sb}_{0.2}$ (cold worked)

Fig. 13(a)

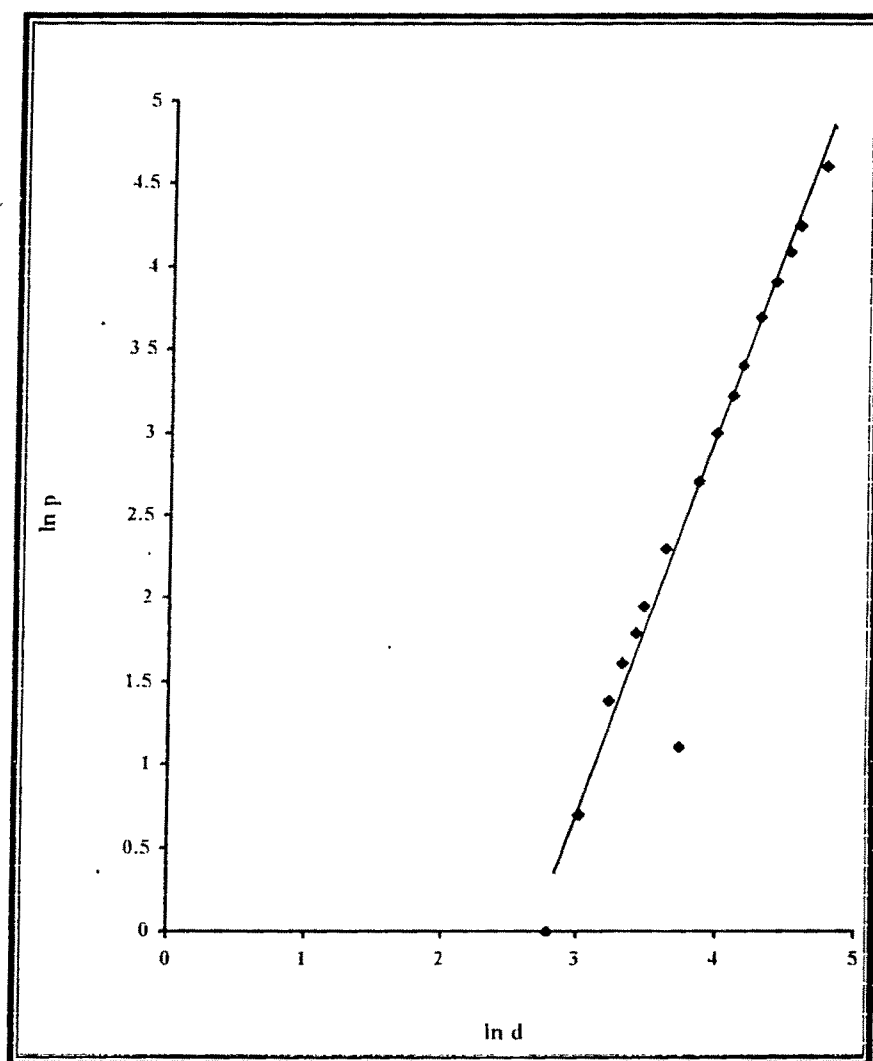
$\text{InBi}_{0.7}\text{Sb}_{0.3}$ (cold worked)

Fig. 13(b)

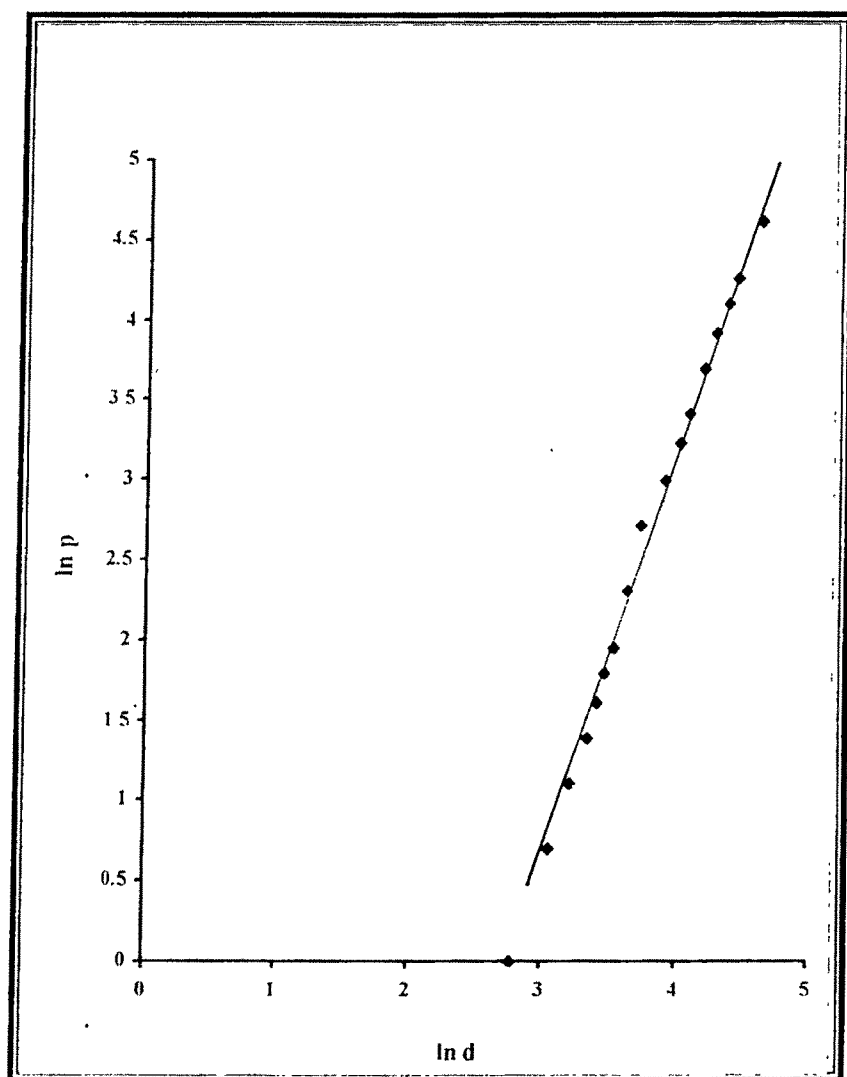
$\text{InBi}_{0.6}\text{Sb}_{0.4}$ (cold worked)

Fig. 13(c)

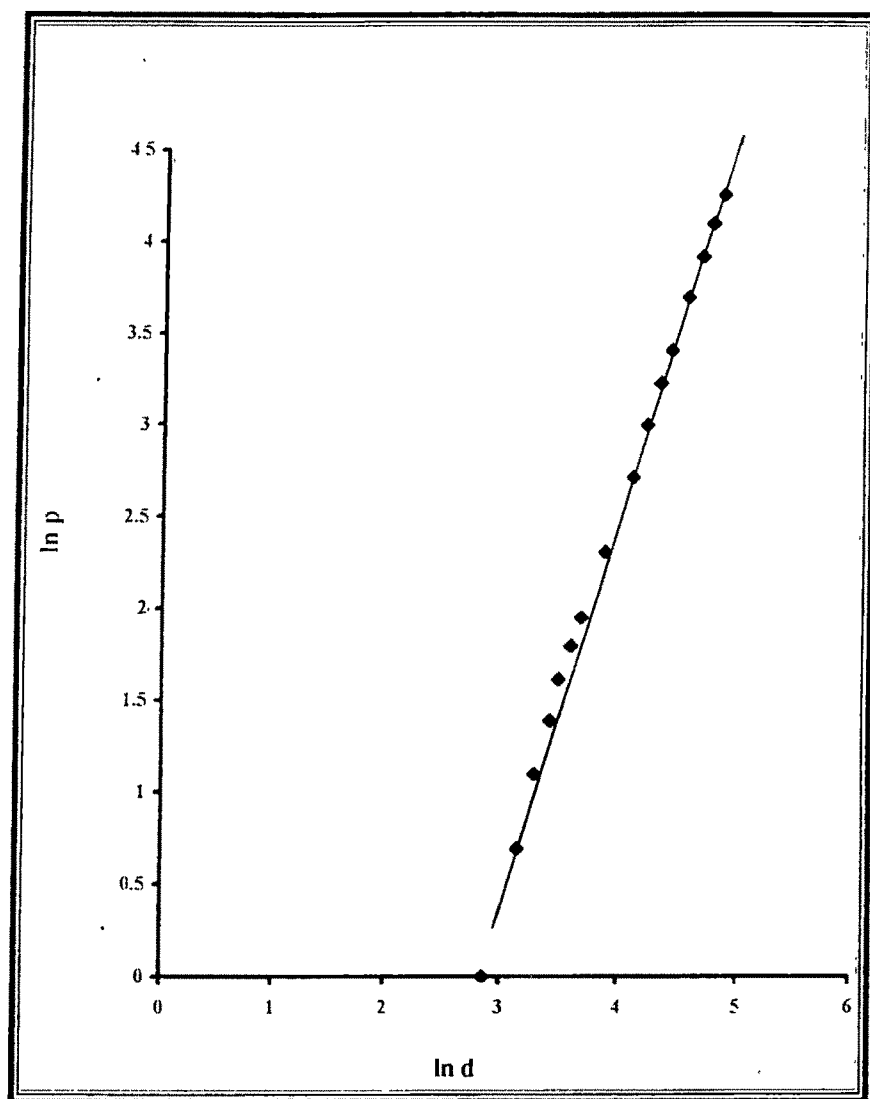
$\text{InBi}_{0.8}\text{Se}_{0.2}$ (as cleaved)

Fig. 14(a)

$\text{InBi}_{0.7}\text{Se}_{0.3}$ (as cleaved)

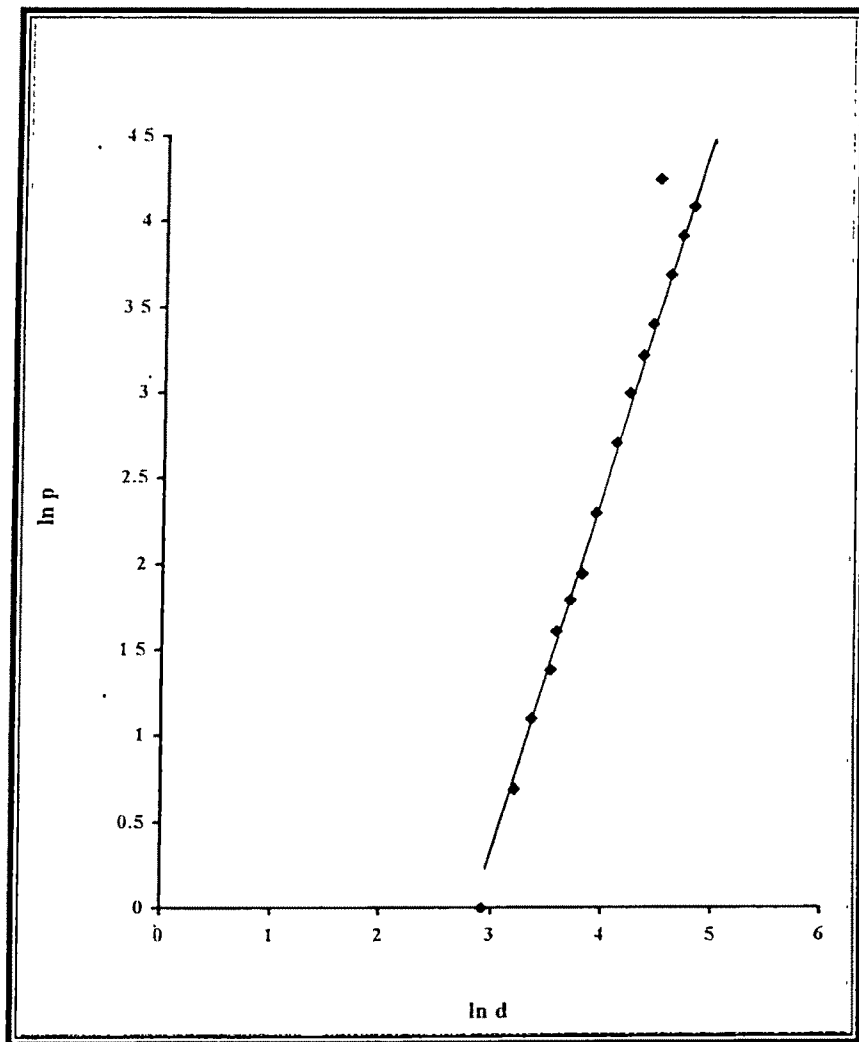


Fig. 14(b)

$\text{InBi}_{0.6}\text{Se}_{0.4}$ (as cleaved)

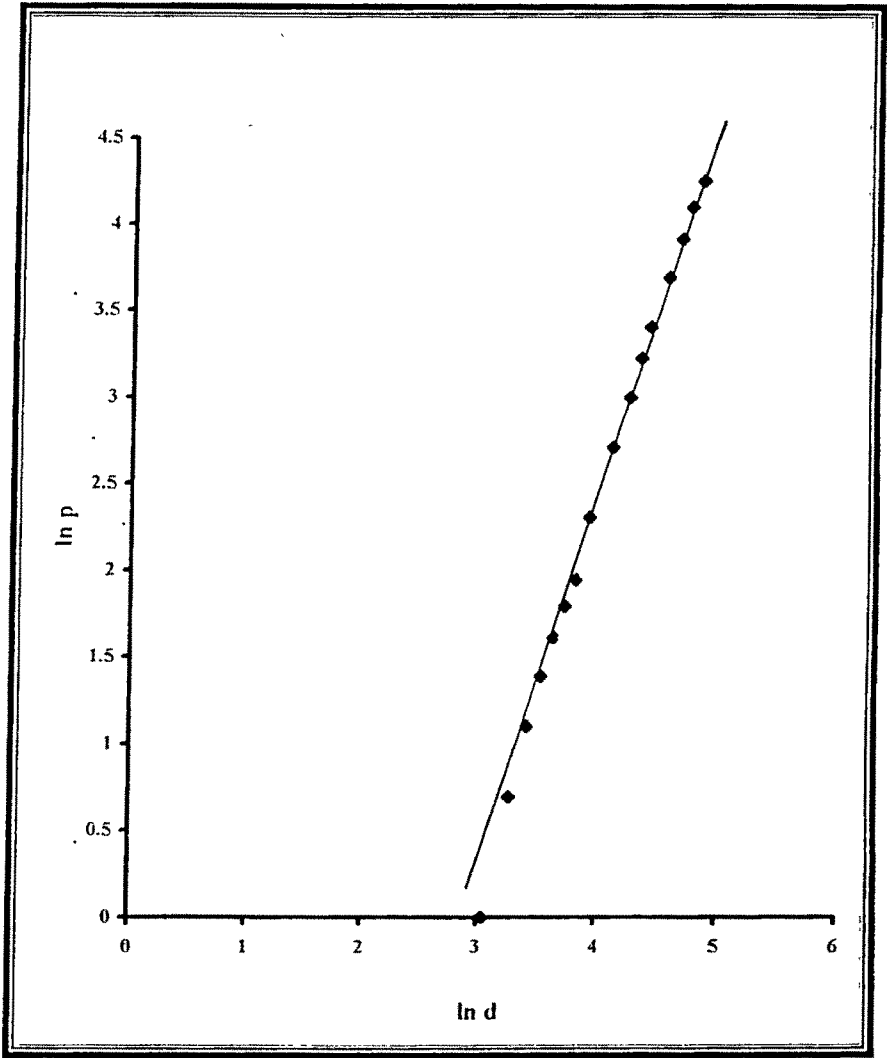


Fig. 14(c)

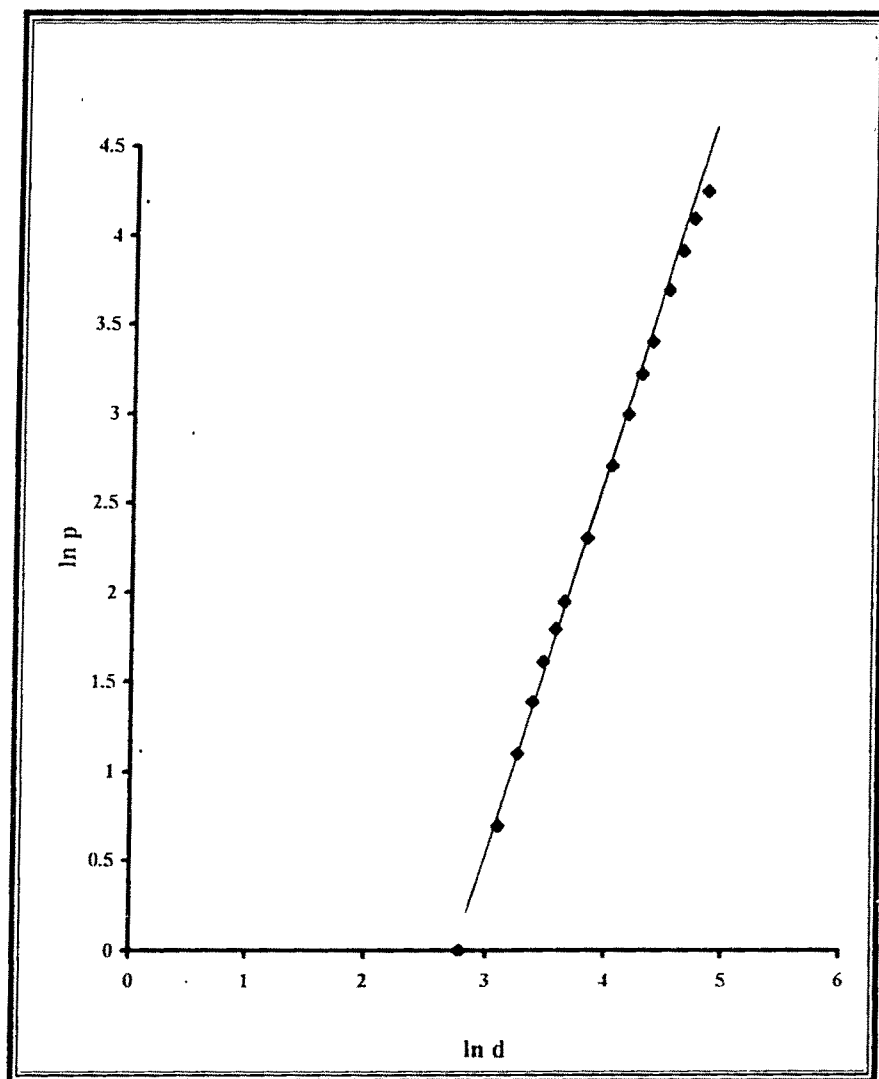
$\text{InBi}_{0.8}\text{Se}_{0.2}$ (cold worked)

Fig. 15(a)

$\text{InBi}_{0.7}\text{Se}_{0.3}$ (cold worked)

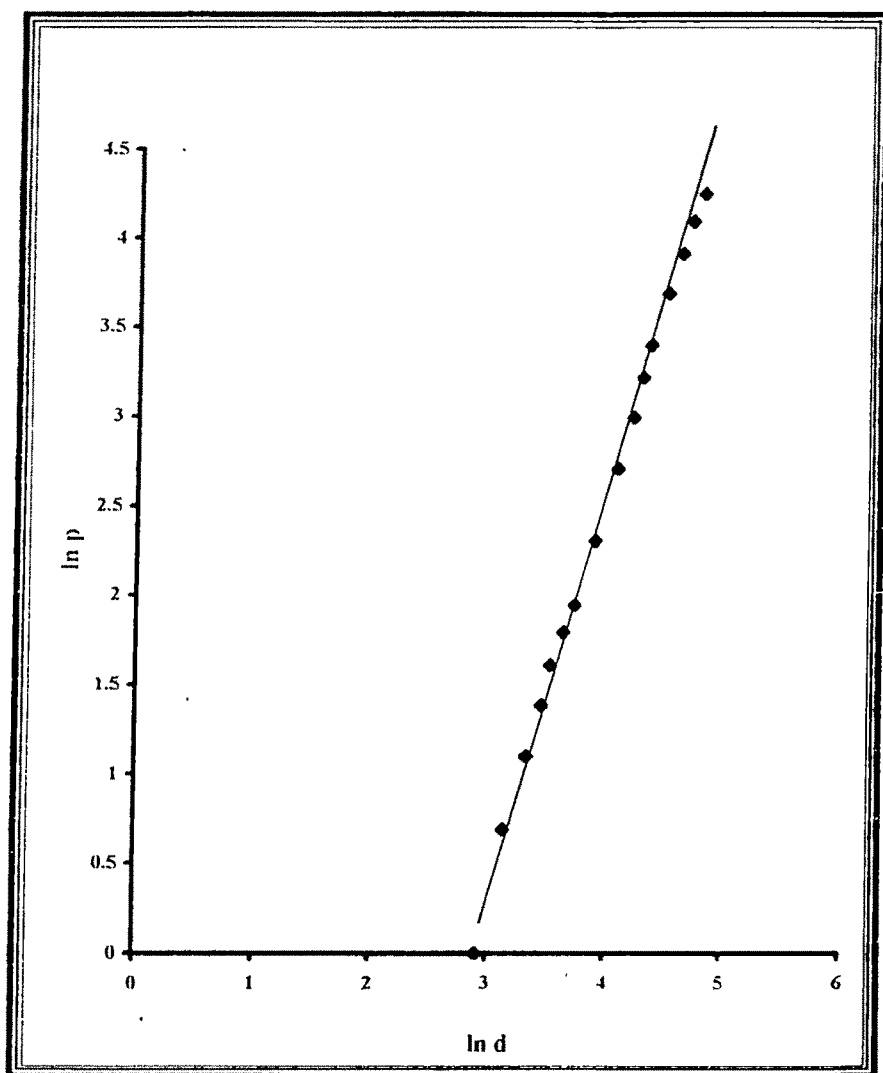


Fig.15(b)

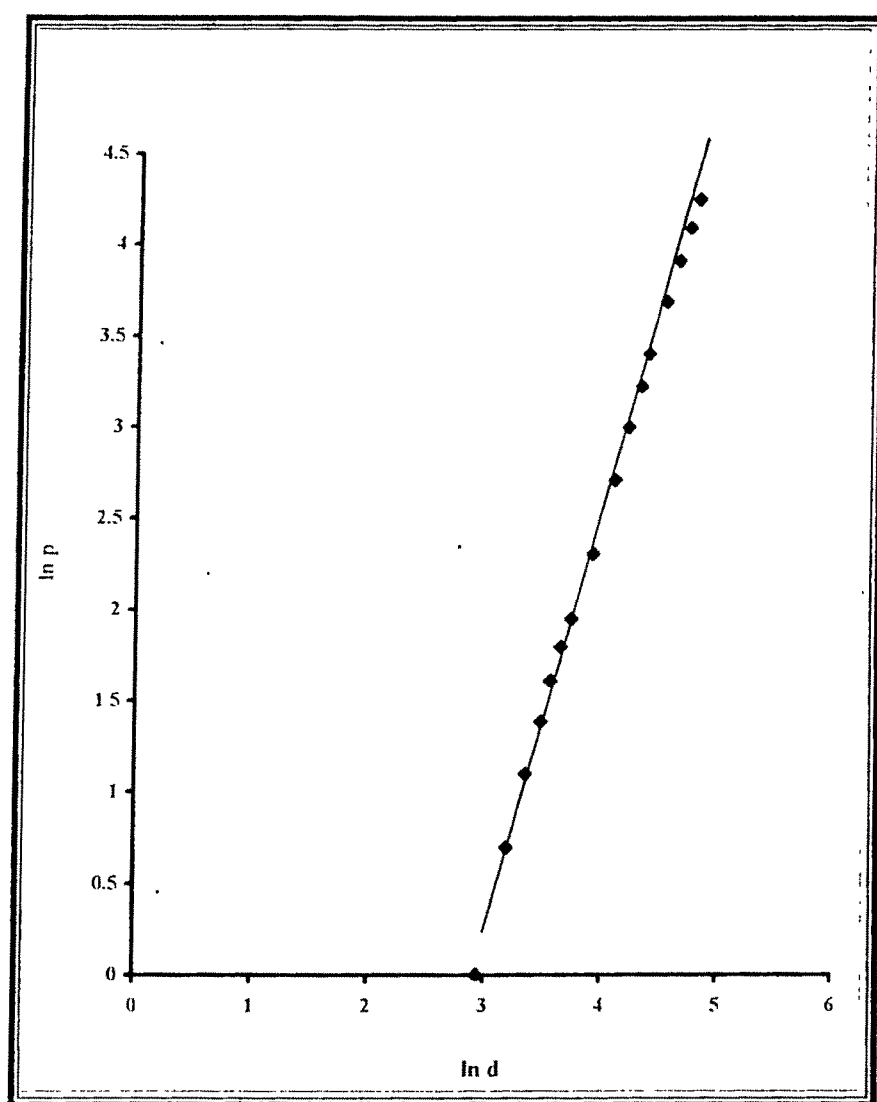
$\text{InBi}_{0.6}\text{Se}_{0.4}$ (cold worked)

Fig. 15(c)

The values of Meyer index obtained in the present case are given in Table-4, for both as-cleaved as well as cold-worked crystals. These values indicate that the load dependence of hardness is quite enhanced in the case of the cold worked crystals. It is interesting to note that the n -value for cold-worked crystal is greater than that for the untreated (as-cleaved) crystals indicating that the work hardening makes the hardness more dependent on load.

HARDNESS ANISOTROPY :

To study the anisotropy exhibited by $[001]$ planes of the crystals, the directional hardness was determined by producing indentations at various azimuthal orientations of the indenter with respect to the surface over a range of 0° to 180° . The reference 0° orientation was set as described earlier. The crystal was rotated about the indenter axis in steps of 15° while keeping the applied load constant at 50 gm (490 mN) in both the cases and keeping loading time constant at 30 second and 50 second, respectively, for $\text{InBi}_{0.8}\text{Sb}_{0.2}$ and $\text{InBi}_{0.8}\text{Se}_{0.2}$ crystals.

The plots of the measured hardness H_v versus orientation θ are shown in fig.16 and fig.17 for $\text{InBi}_{0.8}\text{Sb}_{0.2}$ and $\text{InBi}_{0.8}\text{Se}_{0.2}$ crystals. From the figures, it can be seen that hardness values repeat periodically at 90° intervals. Also, there are distinct maxima and minima, which are also periodic. Thus, in both the cases the hardness anisotropy corresponds to

Table – 4

Impurity	Concentration X	Meyer index n	
		As – cleaved	Cold - worked
Sb	0.2	2.2	2.3
	0.3	2.2	2.4
	0.4	2.2	2.6
Se	0.2	2.1	2.3
	0.3	2.2	2.4
	0.4	2.2	2.4

$\text{InBi}_{0.8}\text{Sb}_{0.2}$

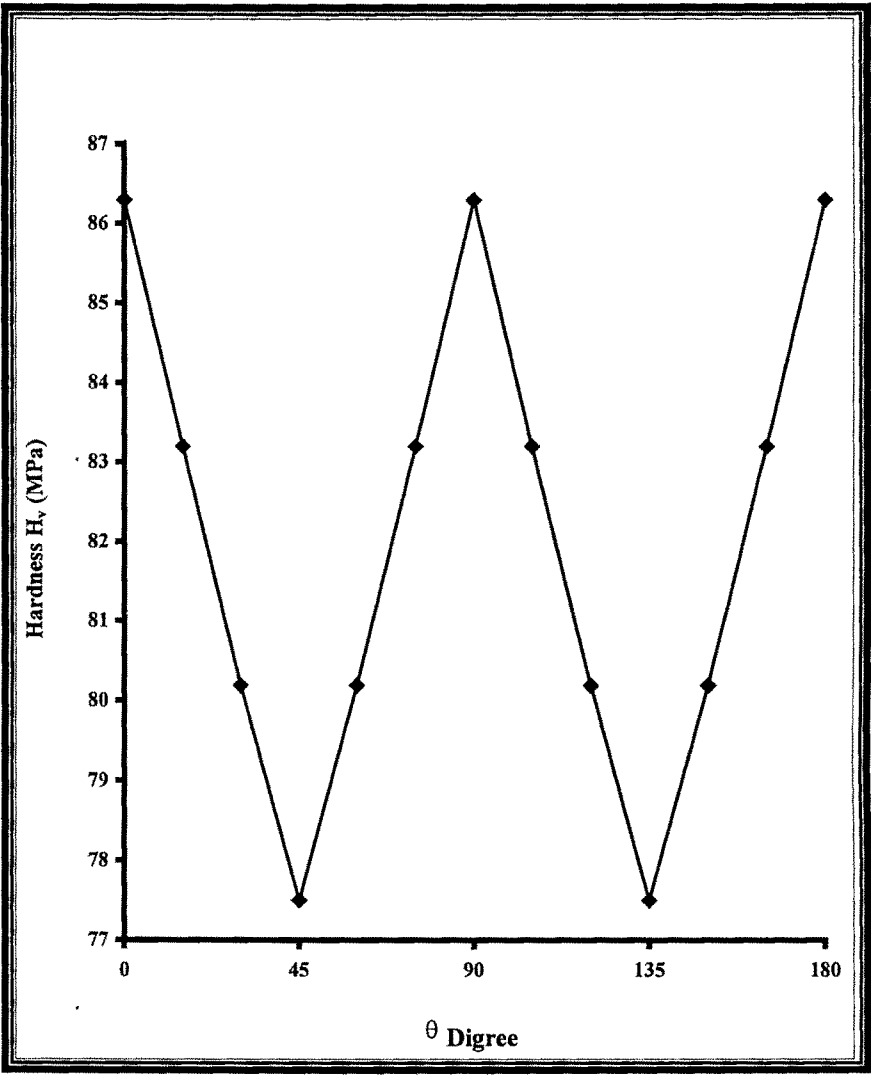


Fig. 16

$\text{InBi}_{0.8}\text{Se}_{0.2}$

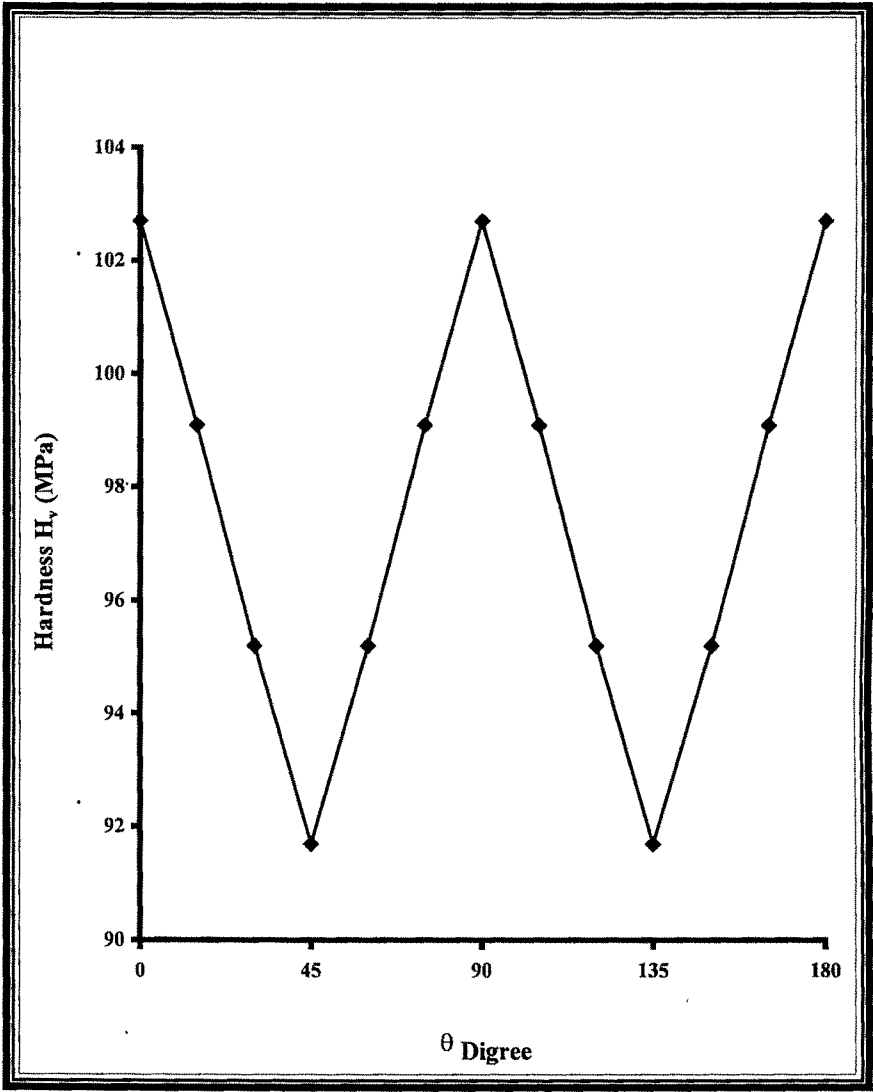


Fig. 17

the four-fold symmetry of the indenter. The crystals have four fold symmetry axis normal to the cleavage planes and hence parallel to the indenter axis. Therefore in this case the symmetry of the indenter, namely, the four-fold axis incorporates the symmetry axis of the crystal. The resulting symmetry in the hardness anisotropy thus does not distinguish the existence of four-fold symmetry of the crystals. It is known that the resolved shear stress produced by the applied force on the slip systems in a crystal is a function of orientation of the force axis relative to the slip planes and directions. Therefore certain orientations are favorable for the indenter to produce deformation as compared to other orientations. In view of this, the hardness peaks observed above occur at such favorable orientation, whereas the minimum corresponds to the least favorable orientations. Ratio of maximum hardness to minimum hardness is found to be 1.12 in the case of $\text{InBi}_{0.8}\text{Sb}_{0.2}$ (Fig.16) and 1.11 in the case of $\text{InBi}_{0.8}\text{Se}_{0.2}$ (Fig.17). Thus the degree of hardness anisotropy is the same for these two crystals.

CONCLUSION :

1. Hardness of $\text{InBi}_{1-x}\text{Sb}_x$ increases with x , whereas for $\text{InBi}_{1-x}\text{Se}_x$ the hardness remains nearly constant with x .
2. For both the crystals, hardness is dependent on load in the low load range.
3. For $\text{InBi}_{1-x}\text{Sb}_x/\text{Se}_x$ ($x = 0.2$) crystals, grown with 30 zone levelling passes, it is observed that the hardness decreases compared to that of crystals grown with 8 zone levelling passes. This has been explained to be a result of improved perfection.
4. The cold working treatment increases the hardness of the crystals.
5. The Meyer index analysis indicates the load dependent nature of hardness of both $\text{InBi}_{1-x}\text{Sb}_x / \text{Se}_x$ crystals.
6. The surface anisotropy of hardness of these crystals is in correspondence with the symmetry of the crystals. Both Sb & Se doped crystals exhibit nearly the same degree of this anisotropy.

REFERENCES

1. Shaw, M.C., The Science of Hardness Testing and Its Research Applications, eds. J.H. Westbrook and H. Conrad (ASM, Ohio), (1973)
2. Tabor, D., The Hardness of Metals (Oxford Univ.), (1951)
3. Bergsman, E.B., Met. Progr., 54 (1948) 153
4. Rostoker, W., J.Inst. Met., 77 (1950) 1975
5. Buckle, H., Rev. Metall., 48 (1951) 957
6. Grodzinsky, P., Indust. Diam. Rev., 12 (1952) 209, 236
7. Knoop, F., Peters, C.G. and Enerson, W.B., J. Res. Nat. Burstand, 23 (1939)
8. Bernhardt, E.D., E.O.Z. Metallik, 33 (1941) 135
9. Campbell, R.F., Henderson, O. and Danleavy, M.R., Trans. ASM, 40 (1948) 954
10. Mott, B.W., Ford. S.D. and Jones, I.R.W., A.E.R.E. Harwell Report, 1R, 1 (1952) 017
11. Taylor, E.W., J. Inst. Met., 74 (1948) 493
12. Toman, L. Jr., Nye, W.F. and Gelas, A.J., 5th Int. Cong. Electron microscopy, 1 (1962) FF – 13
13. Berzina, I.G., Berman, I.B. and Savintsev, P.A., Sov. Phys. Cryst., 9 (1965) 483
14. Gane, N. and Cox, J.M., Phill. Mag., 22 (1970) 881

29. Braunovic, The Sci. of Hardness Testing and its Research Applications eds. By Westbrook and Conrad H., (ASM, Ohio) (1973) 329
30. Vyas S.M., Pandya G.R., Desai C.F., Ind. J. of Pure and appl. Phys., 33 (1955) 191 – 194
31. T. M. Jani, G. R. Pandya. C.F. Desai Cryst. Res Technol. 29 (1994) 1
32. Chen and Hendrickson, Sci of Hardness Testing and Its Applications, Eds. Westbrook and Conrad (ASM, Ohio), (1973) 274
33. Hanemann, H.Z., Metallk, 33 (1941) 124
34. O'Neill, H., The Hardness of Metals and Its Measurements (North Holland)
35. Trivedi, M.D., Ph.D. Thesis, M.S. Univ. of Baroda, (1977)